FlexScatter: Predictive Scheduling and Adaptive Rateless Coding for Wi-Fi Backscatter Communications in Dynamic Traffic Conditions

Xin He, *Member, IEEE*, Jingwen Xie, Aohua Zhang, Weiwei Jiang, Yujun Zhu, Tad Matsumoto, *Life Fellow, IEEE*

***Abstract*—The potential of Wi-Fi backscatter communications systems is immense, yet challenges such as signal instability and energy constraints impose performance limits. This paper introduces FlexScatter, a Wi-Fi backscatter system featuring a designed scheduling strategy based on excitation prediction and rateless coding to enhance system performance. Initially, a Wi-Fi traffic prediction model is constructed by analyzing the variability of the excitation source. Then, an adaptive transmission scheduling algorithm is proposed to address the low energy consumption demands of backscatter tags, adjusting the transmission strategy according to predictive analytics and taming channel conditions. Furthermore, leveraging the benefits of low-density parity-check (LDPC) and fountain codes, a novel coding and decoding algorithm is developed, which is tailored for dynamic channel conditions. Experimental validation shows that FlexScatter reduces bit error rates (BER) by up to 30%, enhances energy efficiency by 7%, and overall system utility by 11%, compared to conventional methods. FlexScatter's ability to balance energy consumption and communication efficiency makes it a robust solution for future IoT applications that rely on unpredictable Wi-Fi traffic.**

***Index Terms*—Wi-Fi Backscatter Communication Systems, Traffic Prediction, Coding Algorithm, Transmission Scheduling, Deep Learning**

I. Introduction

Recent advancements in Internet of Things (IoT) technologies have brought backscatter communication to the forefront as a promising solution for energy-efficient data transmission, leveraging existing environmental radio frequency sources. A standard backscatter communication system consists of an excitation source, tags, and a receiver. These tags modulate and reflect signals from the excitation source to the receiver without regenerating their own signals, allowing tags to operate at ultra-low power levels, typically in the microwatt range.

Ambient backscatter communication, which utilizes ambient radio signals from devices such as Wi-Fi routers and TV transmitters, is favored over dedicated systems due to its lower deployment costs and the ubiquity of signal sources [1]–[4]. The pervasive nature of Wi-Fi signals, in particular, provides substantial advantages for deployment in varied settings like shopping malls and residential areas.

However, the intermittent nature of Wi-Fi signals, governed by protocols such as IEEE 802.11a/g/n, brings significant challenges in maintaining continuous data transmission for backscatter systems [5]. The challenges include variable silent periods between transmissions, which can destabilize the communication link and increase packet loss in backscatter communications. Additionally, the inherent low-power characteristic of backscatter tags restricts their ability to adapt to fluctuating signal availability and interference from other environmental signals.

To address these challenges, this article introduces FlexScatter, a system designed to enhance the performance of Wi-Fi backscatter systems by leveraging predictive modeling of Wi-Fi signals. The main contributions of this paper are summarized as follows:

- Adaptive backscatter scheduling: The paper introduces an adaptive transmission scheduling algorithm that dynamically adjusts transmission strategies based on real-time Wi-Fi traffic predictions. This improves energy efficiency and communication reliability in unpredictable Wi-Fi environments.
- Wi-Fi traffic prediction: We use deep learning to predict Wi-Fi traffic patterns. These predictive models enhance the adaptability of backscatter communication, enabling dynamic adjustments to variations in Wi-Fi traffic.
- We integrate low-density parity-check (LDPC) codes with the principles of fountain codes, using omnipresent Wi-Fi signals for efficient and reliable data transmission. This approach adapts to varying channel conditions by adjusting the encoded packets or bit rates, ensuring optimal use of transmission resources.

The rest of this paper is organized as follows. Section II introduces related work. Section III describes the system architecture adopted in this study. In Section IV, the proposed methods are detailed. Section V presents the experimentally verified results and analysis, comprehensively evaluating the effectiveness of the proposed methods. Finally, Section VI summarizes the entire paper with concluding remarks.

This work was supported by the Natural Science Foundation of China under grants No. 62402229, and 62072004. Corresponding author: *Yujun Zhu*.

X. He, A. Zhang, J. Xie, and Y. Zhu are with the School of Computer and Information, Anhui Normal University, 241002, Anhui, China (e-mail: {xin.he, zhuyujun, zhangaohua, jingwen.xie}@ahnu.edu.cn).

W. Jiang is with the School of Computer Science, Nanjing University of Information Science and Technology, 210044, Jiangsu, China (e-mail: weiwei.jiang@nuist.edu.cn).

T. Matsumoto is with IMT Atlantique, CNRS UMR 6285, Lab-STICC, Brest, France, JAIST, and the University of Oulu (e-mail: matumoto@jaist.ac.jp).

II. The State-of-the-Art

A. Backscatter Communications

Thanks to the significant efforts made by the research community, backscatter communications have been enabled over various radio signals. A breakthrough work in ambient backscatter communication is introduced in [3], where a prototype was developed to transmit information via television signals using backscatter. LoRa backscatter [6] and PLoRa [7] enable long-range backscatter communication using LoRa signals as the excitation signal, where the frequency characteristics of the chirp signal are effectively utilized. FM backscatter [8], which uses continuous FM radio signals as the excitation, has a variety of new applications in urban areas.

Wi-Fi-based backscatter communication has seen considerable development as well. BackFi [9] operates backscatter communications over the Wi-Fi excitation signals transmitted from Wi-Fi access points with hardware modification. Wi-Fi backscatter [10] connects the RF-powered devices to the Internet excited by a Wi-Fi signal. Passive Wi-Fi demonstrates for the first time that it can generate 802.11b backscatter transmissions using backscatter tags [11]. HitchHike [12] enables the backscatter communication over 802.11b signals of the off-the-shelf Wi-Fi transceivers using a proposed codeword translation technique. A more recent work [13] enables per-symbol and in-band backscatter communication over the Wi-Fi excitation signals using a so-called flicker detector by utilizing the residual channel knowledge of the Wi-Fi packets. Furthermore, backscattering of ultra-wideband signals is considered in [14], and X-Tandem [15] enables a multi-hop backscatter system using Wi-Fi signals as excitation sources.

However, these systems have rarely considered how uncontrolled Wi-Fi traffic can be used effectively as an excitation signal. Bitalign [16] achieves 1.98 Mbps throughput and a 0.5% bit error rate by optimizing synchronization and managing uncontrolled signals, providing valuable insights into improving backscatter system reliability. Nti *et al.* [17] introduce nonsequential link adaptation with repetition codes for Wi-Fi backscatter, improving throughput and reliability through a testbed-validated framework. To enable more flexible backscatter communications, the inherent nature of the excitation signal must be taken into account. GuardRider [18], [19] system aims at the effective utilization of the backscatter information in real Wi-Fi networks. However, it assumes that the Wi-Fi signaling duration follows Pareto distributions without verifying the correctness of the actual Wi-Fi traffic characteristics. Yang *et al*. propose a cooperative ambient backscatter communication (CABC) system [20], which optimizes maximum likelihood (ML) and successive interference cancellation (SIC) detectors for OFDM-based backscatter, improving detection performance while reducing system complexity through spectrum sharing. RapidRider [21] system embeds the tag's data into a single OFDM symbol to reduce the effects of uncontrolled Wi-Fi traffic.

B. Overview of Traffic Prediction Techniques

Traffic prediction in wireless networks is broadly categorized into model-driven and data-driven approaches.

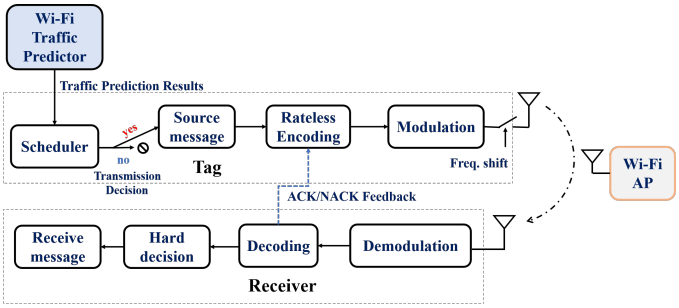

Fig. 1. The proposed system model of Wi-FI backscatter communications with rateless encoding and traffic-based scheduling.

1) Model-driven approaches: These methods model traffic as a statistical process and predict based on predefined distributions. For instance, ref. [22] treats wireless traffic as an unstable process and utilizes a statistical model based on a-stable processes for prediction. This method is particularly suitable for handling abrupt changes in self-similar traffic patterns, which are common in wireless networks.

2) Data-driven approaches: In contrast, data-driven approaches rely on historical traffic data for the predictions, often employing time series analysis and machine learning techniques. Ref. [23] indicates that autoregressive integrated moving average (ARIMA) models could predict regular components, but random components are complex due to low intercorrelation. Ref. [24] successfully predicts the arrival times of wireless network traffic using a random forest regression algorithm, outperforming traditional linear models. Refs. [25] and [26] verify that long short-term memory (LSTM) and other recurrent neural networks outperform conventional statistical methods like ARIMA in predicting network traffic. Ref. [27] makes further advancement of the traffic estimation by employing an LSTM-based framework to predict packet arrival times, enabling more effective dynamic scheduling in wireless networks. Hence, in this work, we implement the Wi-Fi traffic predictor using a deep-learning method.

III. System Architecture

A. System Overview

Most existing Wi-Fi-based backscatter communication systems assume that the excitation source is controllable and continuous. However, to facilitate the practical deployment of the systems, it is necessary to address both intermittent WiFi signal transmission and strong interference.

As shown in Fig. 1, FlexScatter consists of three main components: a Wi-Fi traffic predictor, a customized tag, and a receiver. The Wi-Fi traffic predictor provides input to a scheduler in the tag, determining whether or not to transmit the source message based on the predicted traffic. If the transmission is decided, the source message is channel-encoded using a rateless coding technique, which ensures efficient and reliable data transmission even under varying channel conditions. The encoded message is then modulated and transmitted by the tag, with a 20 MHz frequency shift. The "roadside" Wi-Fi access point (AP) acts as the excitation source for the backscatter communication. At the receiver, the signal is demodulated

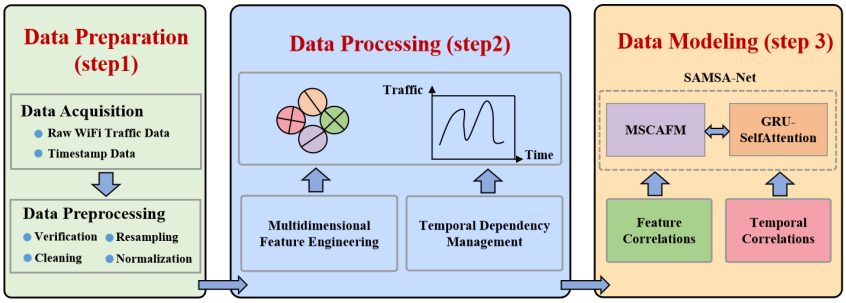

Fig. 2. The workflow of the proposed method for Wi-Fi traffic prediction.

and decoded, with a hard decision block determining the final message. The system also incorporates an ACK/NACK feedback loop between the receiver and the tag, which further enhances communication reliability by allowing for a rateless coding concept.

However, due to the ultra-low power consumption design of the tags, the Wi-Fi traffic predictor is implemented on the receiver side rather than on the tag itself. The receiver, after predicting the traffic, communicates its decision to the tag by sending a two-bit ACK signal—either '11' or '00'—to notify the tag of whether or not to proceed with the transmission. The use of a two-bit signal, instead of a one-bit signal, is crucial for improving the detection reliability at the low-power tag, ensuring that the tag can correctly interpret notifications of the receiver instructions even under challenging power constraints. This design concept enhances the overall efficiency and robustness of the FlexScatter system, particularly in scenarios where energy consumption is of crucial importance.

B. Wi-Fi Traffic Predictor

To implement the Wi-Fi traffic predictor, we employ a deep-learning-based approach leveraging a multi-scale channel attention mechanism. This algorithm leverages previously stored traffic data to train a model capable of making accurate predictions about future Wi-Fi traffic patterns, adapting to complex and dynamic network conditions. By focusing on this approach, the system is designed to effectively balance accuracy and computational efficiency, catering to different timing scales and performance requirements.

The algorithm consists of three key stages: data preparation, data processing, and data modeling, as illustrated in Fig. 2.

1) Data Collection: We collected Wi-Fi traffic data with the Edimax EW-7811Un Wi-Fi card, capturing data through the *tcpdump* tool on a configured computer setup. Each card was assigned to one of the three non-overlapping 2.4 GHz channels (Channels 1, 6, and 11) to ensure comprehensive data collection without interference. Typically, the captured data contains the following features with different scales: time stamp, frame length (bytes), radio duration (μs), interval time (s), data rate (Mbps), and signal strength (dBm). The purpose of the traffic predictor is to estimate the future interval time using these features.

To validate the intermittent transmission of the Wi-Fi signal in real-world environments, we conducted measurements in three representative scenarios: a shopping mall, a laboratory, and a home apartment. These scenarios represent environments with varying traffic densities and practical deployment conditions for backscatter communication systems. Table I summarizes major specifications of the data collection settings, including the area size and the number of access points (APs) on each channel.

TABLE I
DETAILS AND SETTINGS OF WI-FI TRAFFIC DATA COLLECTION SCENARIOS

Scenario	Area (m^2)	Number of APs
Shopping Mall	8000	4 (Ch. 1), 2 (Ch. 6), 3 (Ch. 11)
Laboratory	200	5 (Ch. 1), 3 (Ch. 6), 4 (Ch. 11)
Home Apartment	140	1 (Ch. 1), 2 (Ch. 6), 1 (Ch. 11)

Among these scenarios, the shopping mall (Channel 6) was selected as the representative high-traffic environment for further analysis. This environment exhibited consistent and dense traffic activity, making it suitable for studying the intermittent transmission of the Wi-Fi signal and its impact on backscatter communication systems.

Recognizing the potential for discrepancies due to device failures or malfunctions from various monitoring setups, we conduct a preprocess to refine the raw data beforehand.

2) Data Preparation: The preprocessing begins with a detailed inspection of the dataset to identify and rectify issues such as irrelevant or unquantifiable parameters, missing values, and outliers. We then slice the data into clusters using 1 second per cluster. Particular attention is paid to the intervals between clusters of Wi-Fi data as shown in Fig. 3. Following the initial cleanup, we transform the dataset to feature uniform time intervals, enhancing the consistency and analytical viability for subsequent time series evaluations. Finally, we implement a min-max normalization strategy, adjusting all feature values to a $[0, 1]$ range, which normalizes the data, facilitating more effective comparisons and analyses in the later stages.

3) Data Processing: The goal of Wi-Fi traffic flow prediction refers to the process of predicting the on/off state in the future based on the time series of Wi-Fi traffic data, that is, using the data of the current time t to estimate the Wi-Fi traffic at the next time $t + \Delta t$. Furthermore, to meet the requirements of applications including Wi-Fi backscatter communications, we aggregate predictions over future time steps Δt to estimate overall trends. The reason is twofold; First of all, by aggregating the values within Δt, a more accurate prediction is achieved. Then, it is extremely power-consuming

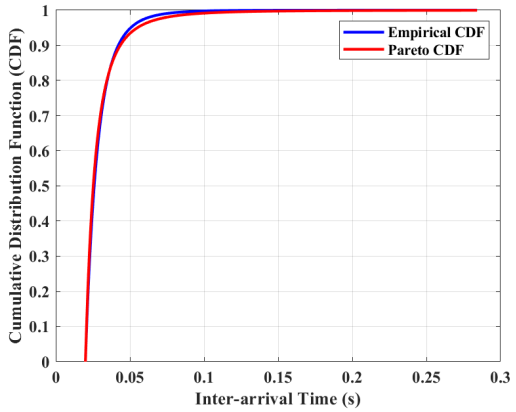

(a) CDF Comparison

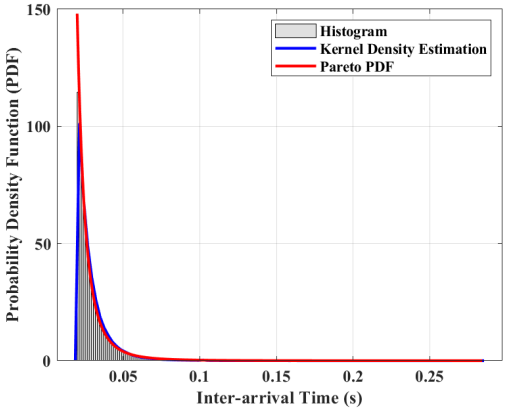

(b) Data Distribution with

Fig. 3. Analysis of interval time data with Pareto distribution.

for the tag to adjust the transmission frequently within a short time period.

4) Data Modeling: We design a deep learning model based on the multi-scale channel attention fusion module (MSCAFM) to predict Wi-Fi traffic while considering temporal factors accurately. The model implementation comprises three key stages: multidimensional feature extraction, temporal factor fusion, and sequence prediction.

In the multidimensional feature extraction stage, SAMSA-Net leverages MSCAFM to capture multi-scale temporal features of Wi-Fi traffic data. It combines the squeeze-and-excitation (SE) attention mechanism and gating units to optimize the representation and integration of the selected features, establishing a robust feature foundation for sequence prediction.

During the temporal factor fusion stage, the model incorporates long-term time stamps (such as hours and weekdays) as features and integrates them with traffic data through attribute feature units (AF-units). It enhances the sensitivity of the model to temporal variations, improving prediction accuracy and real-time performance.

Finally, in the sequence prediction stage, SAMSA-Net processes the integrated feature matrix using gated recurrent units (GRU) and self-attention mechanisms. It enables the model to effectively capture long- and short-term trends in traffic data, which enhances the prediction accuracy.

C. Scheduler

The designed scheduler is to enhance data transmission reliability and efficiency under varying Wi-Fi conditions. The algorithm dynamically adjusts its strategy based on the Wi-Fi traffic conditions estimated in real-time, by the Wi-Fi traffic predictor, effectively managing transmission intervals to alleviate large interference and optimizing both network reliability and energy conservation.

Real-time Wi-Fi traffic data is collected for the current period and used to predict future traffic values for the next Δt seconds based on the past L time steps. In the following experiments, multiple Δt time step predictions are summed up to estimate overall trends and traffic levels. Experiments indicated that using $L = 64$ and $\Delta t = 5$ provide the best predictive performance. After that, we compare the predicted Wi-Fi interval rate with a predefined threshold W_I. If the predicted value is under W_I, then the tag will backscatter its message. Otherwise, the tag keeps silent to save energy.

D. Rateless LDPC Coding

For the channel-encoding process, the tag implements LDPC coding with an infinite code rate, focusing on a well-designed check matrix construction and adaptive encoding and decoding processes.

1) Index matrix construction: LDPC codes utilize parity check matrices for encoding. To adapt to infinite code rates, we dynamically generate various index matrices by modifying initial exponent values in the index matrix, as

$$\mathbf{P} = \begin{pmatrix} a^{\mathbf{x}}b^{\mathbf{y}} & a^{\mathbf{x}+1}b^{\mathbf{y}} & \cdots & a^{\mathbf{x}+m}b^{\mathbf{y}} \\ a^{\mathbf{x}}b^{\mathbf{y}+1} & a^{\mathbf{x}+1}b^{\mathbf{y}+1} & \cdots & a^{\mathbf{x}+m}b^{\mathbf{y}+1} \\ \vdots & \vdots & \ddots & \vdots \\ a^{\mathbf{x}}b^{\mathbf{y}+n} & a^{\mathbf{x}+1}b^{\mathbf{y}+n} & \cdots & a^{\mathbf{x}+m}b^{\mathbf{y}+n} \end{pmatrix} \quad (1)$$

where a and b stand for prime numbers, and $\mathbf{x}$ and $\mathbf{y}$ are discrete random variables characterized by their probability distributions.

These index matrices facilitate encoding with different generator matrices, ensuring continuous transmission of encoded data packets. Fig. 4 shows the simulation results demonstrating bit error rate (BER) performance with the index x as a parameter. It is found that the BER performance is stable over different matrices.

2) Efficient check matrix Design: The system employs a new encoding technique for constructing the parity check matrix of irregular QC-LDPC codes. The check matrix $\mathbf{H}$ consists of two parts, $\mathbf{H}_1$ and $\mathbf{H}_2$, where $\mathbf{H}_1$ is derived from the index matrix, and $\mathbf{H}_2$ includes a shiftable identity matrix $\mathbf{I}$, facilitating the construction of a cycle-free irregular matrix. This structure not only mimics the performance of random LDPC codes but also simplifies the computation with the corresponding generator matrix.

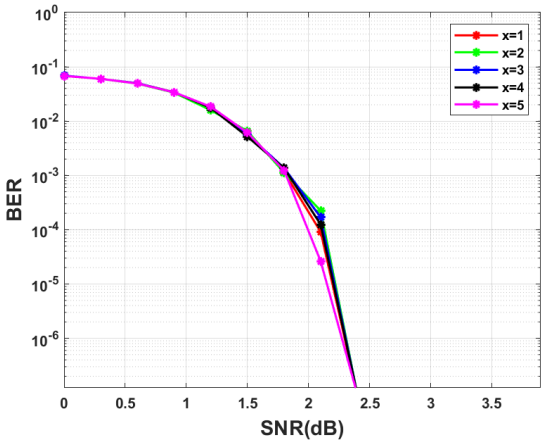

Fig. 4. BER performance with various initial exponent values.

$$\mathbf{H}_1 = \begin{pmatrix} \mathbf{I}_{a^x b^y} & \mathbf{I}_{a^{x+1} b^y} & \cdots & \mathbf{I}_{a^{x+m} b^y} \\ \mathbf{I}_{a^x b^{y+1}} & \mathbf{I}_{a^{x+1} b^{y+1}} & \cdots & \mathbf{I}_{a^{x+m} b^{y+1}} \\ \vdots & \vdots & \ddots & \vdots \\ \mathbf{I}_{a^x b^{y+n}} & \mathbf{I}_{a^{x+1} b^{y+n}} & \cdots & \mathbf{I}_{a^{x+m} b^{y+n}} \end{pmatrix} \tag{2}$$

$$\mathbf{H}_2 = \begin{pmatrix} \mathbf{I} & \mathbf{I} & 0 & \cdots & 0 & 0 \\ 0 & \mathbf{I} & \mathbf{I} & \cdots & 0 & 0 \\ \vdots & \vdots & \vdots & \ddots & \vdots & \vdots \\ \mathbf{I} & 0 & 0 & \cdots & 0 & 0 \\ 0 & 0 & 0 & \cdots & 0 & 0 \\ \vdots & \vdots & \vdots & \ddots & \vdots & \vdots \\ 0 & 0 & 0 & \cdots & \mathbf{I} & \mathbf{I} \\ \mathbf{I} & 0 & 0 & \cdots & 0 & \mathbf{I} \end{pmatrix} \tag{3}$$

After constructing the parity check matrix $\mathbf{H}$, it is converted into a standard form $[\mathbf{I}|\mathbf{Q}]$ through row-wise Gaussian elimination. Consequently, the generator matrix $\mathbf{G}$ is formed as $[\mathbf{P}|\mathbf{I}]$, where $\mathbf{P} = \mathbf{Q}^T$.

3) Adaptive encoding and decoding of LDPC: Unlike traditional LDPC coding, our method adopts feedback from the receiver to notify the transmitter of the encoding strategies. The tag in the system dynamically adapts encoding processes based on feedback. Positive feedback leads to successive information frame encoding, while negative feedback (NACK signals) prompts the regeneration of new index and generator matrices for re-encoding the failed frames. This adaptive encoding approach enhances the resilience of data transmission.

4) Enhanced decoding with improved BP algorithm: Our decoding strategy incorporates an improved Belief Propagation (BP) algorithm, which utilizes saved decoding results from previous iterations to further refine decoding accuracy in subsequent attempts. This iterative process effectively reduces BER and ensures reliable data transmission over noisy channels.

Specifically, the algorithm flow is shown in Algorithm 1, where *BPfunction* represents the improved BP algorithm, and the normalization function represents the normalization algorithm. Let the code length of a single encoded packet be N, and let M be the half of the code length. Thus, $L(Q_i)$ represents the parity bits of the encoded packet, and $L(C_i)$ represents the information bits of the encoded packet.

Algorithm 1 Rateless LDPC Code Decoding Process

Require: Prior probability of observations $L(C_i)$
Ensure: Hard decision for each bit $\hat{x}$

count = 1
while $ACK \neq 11$ **do**
  if count == 1 **then**
    $(ACK, L(Q_i)) =$ BPfunction$(L(C_i))$
  else
    $L(C_i) = [L(C_i)(1:M), L(Q_i)(M+1:N)]$
    Normalization function$(L(C_i))$
    $(ACK, L(Q_i)) =$ BPfunction$(L(C_i))$
  end if
end while
if $L(Q_i) < 0$ **then**
  $\hat{x} = 1$
else
  $\hat{x} = 0$
end if

The improved BP algorithm returns two values: a feedback signal and posterior probabilities.

- The feedback signal is either ACK or NACK, represented by binary 11 and 00, respectively. ACK indicates successful decoding and informs the tag to encode and send the next information frame. Conversely, if the receiver sends a NACK, the tag will continue to use the indexing matrix module and the generator matrix module to construct more generator matrices to re-encode the unsuccessfully decoded information frame and resend it to the receiver.
- The posterior probabilities consist of the probabilities of information bits and parity bits. If decoding fails, the results of the most recent information bits are retained and used to replace the information bits in the next BP algorithm iteration, while the parity bits in the new packet remain unchanged. Therefore, in practical system operation, apart from the first transmission, which requires a complete encoded packet, subsequent transmissions only need to send encoded parity bits if decoding fails.

The normalization algorithm ensures that the results after each BP algorithm iteration are within a certain range to maintain successful decoding. It is particularly important because a high signal-to-noise ratio (SNR) can affect the posterior probability range in the improved BP algorithm, potentially generating erroneous values and leading to decoding failures. In the experiment detailed in the following Section, the normalization algorithm employs a linear function to limit the posterior probability values within the range of -5 to 5.

IV. Experimental Results and Analysis

A. Performance Metrics

Typically, we consider the BER indicating the transmission accuracy. Besides, energy consumption is a crucial factor for the tag requiring ultra-low power consumption. Hence, we

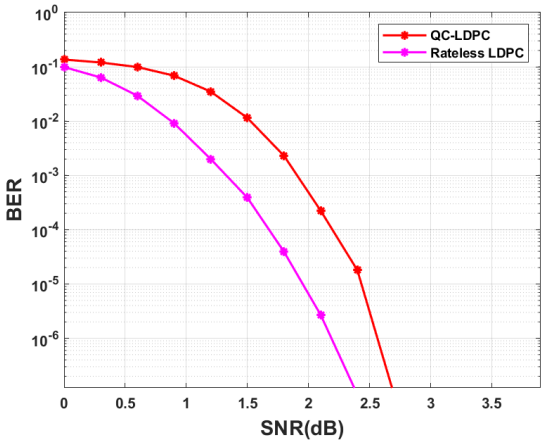

Fig. 5. BER comparison between rateless and QC-LDPC codes across different SNRs.

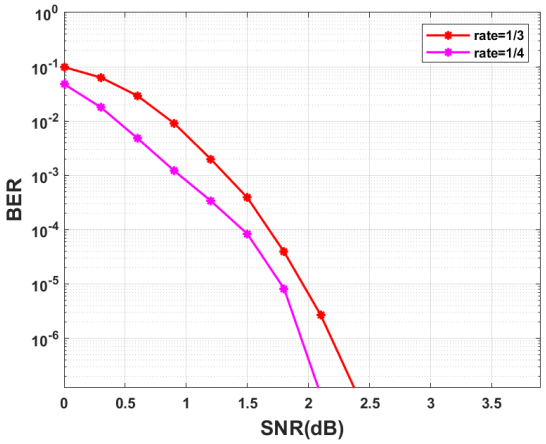

Fig. 6. Effect of adjusting the coding rate on BER of rateless LDPC codes.

jointly consider BER, throughput, and energy consumption when designing a new metric, namely, utility in the backscatter communications.

For evaluating energy efficiency, first of all, based on the ultra-low power consumption characteristics of backscatter communication systems, this paper assumes that each bit transmitted by the backscatter tag consumes 10 μJ of energy. According to Algorithm 1, except for the first transmission, which requires a complete coded packet, subsequent transmissions only need to send parity bits. Therefore, the total energy required to send a coded packet is given by

$$E = 10\left(\frac{N}{2}(n+1)\right), \tag{4}$$

where n represents the total number of packets and N the number of bits in each coded packet.

To describe system performance in terms of how much information is correctly received per unit of time, we adopt throughput as an indicator of reliable transmission performance, defined as:

$$T = R(1 - P_e), \tag{5}$$

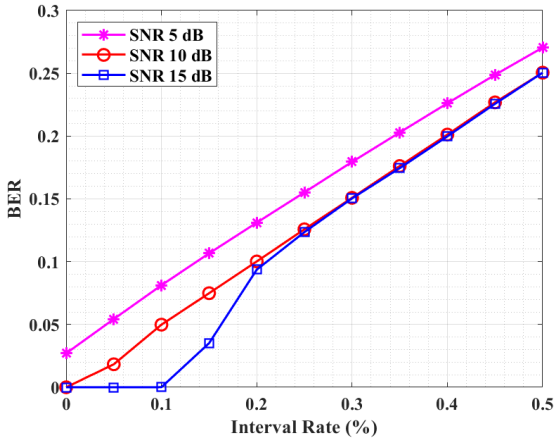

Fig. 7. Performance comparison of different SNR across varied Wi-Fi traffic interval ratios.

where R is the transmission rate at the tag and P_e the BER after n transmissions.

With the energy and throughput metrics, the utility value U is defined to evaluate system performance:

$$U = \frac{\alpha T}{\beta E}. \tag{6}$$

In this work, α and β are set at 1 for a general evaluation.

To make solid evaluations of the system performance, we consider three distinct cases:

- Without scheduling: In this scenario, the system operates without any predictive scheduling, relying solely on the immediate availability of Wi-Fi signals, which may result in suboptimal performance due to the unpredictability of traffic.
- Scheduling using deep learning: Here, the system employs the proposed deep-learning-based algorithm for traffic prediction, enabling it to schedule transmissions more effectively by anticipating Wi-Fi traffic patterns.
- Scheduling using ideal values: In this case, the system uses perfect, idealistic predictions of Wi-Fi traffic (i.e., knowing the exact future traffic conditions). This serves as an upper-bound benchmark, showing the maximum possible performance improvement that could be achieved with perfect prediction.

B. Micro-Benchmark Experiments

1) Evaluation on coding/decoding design: This section evaluates the performance of rateless LDPC codes with different communication scenarios, focusing on BER as the primary performance metric. The experiments are conducted on an additive white Gaussian noise (AWGN) channel to simulate varying noise levels represented by different SNRs.

The simulation transmits 1000 packets in total, with 1310 bits per packet. Each packet is encoded using LDPC with rate $1/2$ and the index matrix parameters being $a = 3$ and $b = 7$.

Initial experiments aim to compare the rateless LDPC codes with conventional QC-LDPC codes. As shown in Fig. 5, the rateless codes consistently outperformed QC-LDPC codes in

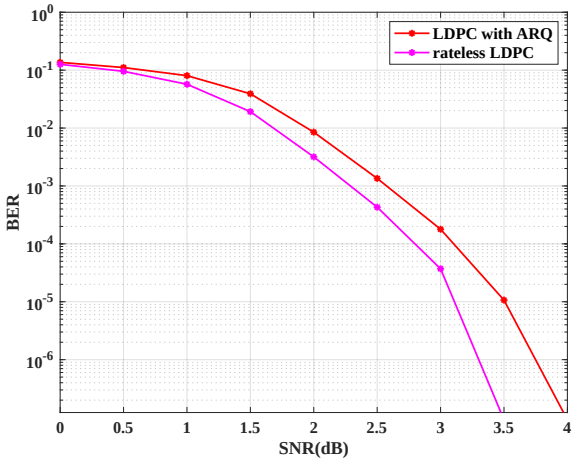

Fig. 8. Performance comparison of rateless LDPC coding and ARQ under varied Wi-Fi conditions.

terms of BER over the entire SNR values tested, demonstrating their robustness in noisy environments.

The simulation then changed the coding rate to evaluate the BER performance sensitivity to the coding rate matching. The results reveal that an increase in the number of transmitted packets notably decreased BER, highlighting the superiority of rateless codes to maintain low error rates, as shown in Fig. 6.

Due to the interval rate of Wi-Fi traffic affecting the performance largely, we adopt a set of Wi-Fi interval ratios to evaluate the performance of rateless LDPC codes. As demonstrated in Fig. 7, the adopted rateless LDPC code could still perform effectively until 20% interval ratios with different SNR values. Hence, we set the threshold of the interval ratio to 20% in the scheduling algorithm.

Lastly, a comparative evaluation against a basic ARQ retransmission mechanism underlined the superior adaptability of rateless LDPC codes to fluctuating network conditions, as shown in Fig. 8. In the ARQ scheme, the construction matrix of the LDPC code remains the same and we just send the same coded packets repeatedly. Compared to the ARQ case, we gain around 0.5 dB in SNR.

These extensive tests validate the superior performance of rateless LDPC codes, making them highly suitable for environments with variable interference and discontinuity of Wi-Fi traffic.

2) Wi-Fi traffics prediction: The Wi-Fi traffic dataset adopted in this study was captured in commercial shopping venues, covering the main operational hours from 9:00 AM to 10:00 PM daily over a week. An 80/20 data split strategy was employed to identify the best model configuration.

A sliding window technique was employed, utilizing the data at the current time t to predict the Wi-Fi traffic at the next timing $t+\Delta t$. The sliding window approach is chosen because it allows the model to capture temporal dependencies in the data, making it particularly effective for time-series prediction. By clustering similar patterns within the window, the model can accurately predict and anticipate future traffic trends.

In the experiments, the model hyperparameters included a learning rate of 0.0001, a batch size of 64, and a training period of 100 epochs. We utilize the Adam optimizer for gradient descent, and all neural network-based methods were implemented using the PyTorch framework due to its flexibility and convenience for deep learning research.

TABLE II
COMPARISON OF EXPERIMENTAL RESULTS UNDER DIFFERENT SETTINGS

Method	MSE	RMSE	MAE
ARIMA	0.027819	0.166790	0.103130
MLP	0.012733	0.112840	0.082369
CNN	0.011440	0.106960	0.084562
LSTM	0.009120	0.095499	0.070014
GRU	0.008823	0.093932	0.062518
CNN-GRU	0.008659	0.093056	0.063019
Our Method	**0.008285**	**0.091021**	**0.061926**

To evaluate the performance of our prediction models, we select three primary performance metrics: mean squared error (MSE), root mean squared error (RMSE), and mean absolute error (MAE).

To demonstrate the superiority and effectiveness of our proposed method, we compare it with several widely used baseline models, including ARIMA, MLP, CNN, LSTM, GRU, and CNN-GRU. The results are summarized in Table II.

The experimental results clearly demonstrate that our deep learning methods significantly outperform the traditional time-series models such as MLP and ARIMA in terms of prediction accuracy for the next $\Delta t = 5$. The results demonstrate that our proposed method can achieve substantial improvements in MSE, RMSE, and MAE compared to these models. Specifically, our method reduces MSE by approximately 70.22%, RMSE by 45.43%, and MAE by 39.95% compared to the ARIMA model; it reduces MSE by approximately 34.93%, RMSE by 19.34%, and MAE by 24.82% compared to the MLP model.

Moreover, when compared with other deep learning models such as CNN, LSTM, GRU, and CNN-GRU, our method also demonstrates superior performance. Our method reduces MSE, RMSE, and MAE by 27.58%, 14.90%, and 26.77% compared to CNN; 9.16%, 4.69%, and 11.55% compared to LSTM; 6.10%, 3.10%, and 0.95% compared to GRU; and 4.32%, 2.19%, and 1.73% compared to CNN-GRU. These results not only assure the effectiveness of our method in the field of deep learning but also highlight its significant advantages in time-series prediction.

3) Impact of Scheduling Threshold: To optimize the scheduling strategy for backscatter tags, we propose halting data transmission when the Wi-Fi interval rate exceeds a predefined threshold to conserve energy. Backscatter tags will resume transmission only when the interval rate is below this threshold. During low interval rates, the number of encoding packets is restricted based on fountain coding principles to efficiently utilize limited energy resources.

We then investigate the utility value variations under different coding rates as the interval rate increases, with a fixed SNR of 10 dB in an AWGN channel. The Wi-Fi interval rate ranges from 0 to 0.5, using a rateless LDPC coding scheme. The maximum number of encoding packets was randomly changed between 2 and 9, and the data transmission rate R was set at 1

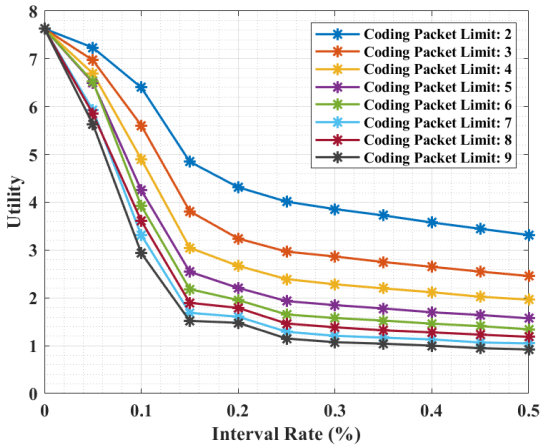

Fig. 9. Comparison of system utility values at different interval rates and different numbers of coding packets.

Mbps. The utility value was used as the primary performance indicator of our design system.

Figure 9 presents utility values against Wi-Fi interval rates with maximum encoding packet limit as a parameter. The utility value curves plateau between interval rates of 15% to 25%. The plateau occurs because the total energy used remains constant as the number of encoding packets needed for reliable transmission increases, leading to stabilization in throughput and utility value.

Increasing the maximum number of encoding packets results in a stable utility value with the same interval rate. This is because each additional packet monotonically increases the transmission energy, while throughput increase diminishes, leading to stable utility value, as shown in (4).

To avoid low utility value regions, it is recommended that the interval rate threshold W_I be set at 25%. Backscatter tags should remain silent when the Wi-Fi interval rate exceeds this threshold and resume transmission when it falls below the threshold. The optimal coding rate is 1/5, and the maximum number of encoding packets should be set to 4, which optimizes the transmission utility.

The configuration of the time slice length Δt and the sliding window size L significantly affect the system performance of the scheduling algorithm, by making a balance of prediction accuracy, computational complexity, and energy efficiency. Experimental results suggest that $\Delta t = 5$ seconds and $L = 64$ achieve an optimal tradeoff under the given conditions.

As shown in Table III, the shorter the time slices, (*e.g.*, $\Delta t = 2$ with $L = 16$), the better the prediction accuracy, with reduced MSE, RMSE, and MAE by 11.89%, 6.10%, and 5.27%, respectively, compared to $\Delta t = 5$ seconds ($L = 64$). The observed improvements are due to the ability of the system to capture rapid traffic variations more effectively. However, the shorter time slices require more frequent scheduling and predictions, which results in significantly higher computational complexity and energy consumption. These factors limit the practicality of such configurations in resource-constrained environments.

Conversely, the longer time slices, *e.g.*, $\Delta t = 10$ seconds with $L = 256$, the smaller the computational complexity but the worse the prediction accuracy. Compared to $\Delta t = 5$ seconds, and $L = 64$, MSE, RMSE, and MAE increase by 25.06%, 11.84%, and 11.08%, respectively. This observation indicates the reduced adaptability of the system in the presence of dynamic traffic fluctuations, resulting in higher error rates and lower reliability.

TABLE III
PREDICTION PERFORMANCE METRICS FOR DIFFERENT TIME SLICE CONFIGURATIONS

Time Slice Duration (Δt) and L	**MSE**	**RMSE**	**MAE**
$\Delta t = 2 \quad (L = 16)$	0.015	0.122	0.098
$\Delta t = 5 \quad (L = 64)$	0.017	0.130	0.103
$\Delta t = 10 \quad (L = 256)$	0.021	0.145	0.114

TABLE IV
SYSTEM PERFORMANCE METRICS FOR DIFFERENT CONFIGURATIONS

Time Slice Length (Δt) and L	**BER**	**Utility**	**Throughput (Mbps)**
$\Delta t = 2\,(L = 16)$	0.12	0.85	0.99
$\Delta t = 5\,(L = 64)$	0.14	0.78	1.00
$\Delta t = 10\,(L = 256)$	0.50	0.39	0.93

From a system performance perspective (see Table IV), $\Delta t = 5$ seconds and $L = 64$ achieve a balanced tradeoff across the key metrics. With this configuration, the system achieves a BER of 0.14, utility of 0.78, and throughput of 1.00 Mbps, providing a good compromise between accuracy, energy efficiency, and system adaptability.

With shorter time slices (*e.g.*, $\Delta t = 2$, $L = 16$), BER is reduced by 14.3% and the utility metric improved by 8.97%. However, the throughput slightly drops by 1.0%, compared to $\Delta t = 5$ seconds. Despite the improvements of the BER and the utility metric, the high energy cost due to frequent scheduling and predictions makes the shorter time slices less practical for real-world deployments.

On the other hand, longer time slices (*e.g.*, $\Delta t = 10$, $L = 256$) result in significant performance degradation. Compared to $\Delta t = 5$ seconds, BER increases by 257.1%, utility decreases by 50.0%, and throughput drops by 7.0%. It verifies that the system can rarely adapt to dynamic traffic patterns in this case, leading to lower reliability and efficiency.

It is important to emphasize that $\Delta t = 5$ seconds and $L = 64$ represent the optimal configuration for the specific experimental conditions tested in this paper. While shorter time slices improve prediction accuracy, their higher computational and energy costs limit their practicality. Conversely, longer time slices reduce energy consumption but sacrifice prediction accuracy and adaptability. Therefore, $\Delta t = 5$ seconds and $L = 64$ provide the best compromise under the given conditions.

C. Macro-benchmark Experiments

This section analyzes the impacts of scheduling strategies using deep learning predictive methods on the performance enhancement of backscatter communication systems. Our simulations were conducted in realistic environments characterized by AWGN with an SNR of 10 dB. The scheduling

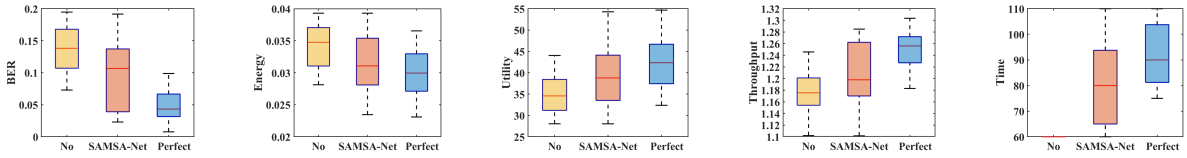

(a) BER (b) energy (c) utility (d) throughput (e) time

Fig. 10. The improvement on the system performance using scheduling driven from deep learning and perfect knowledge. The perfect knowledge is adopted as the optimal performance for performance comparison.

strategies used in the simulations are a 0.25-time slot interval rate threshold and a 1/5 code rate, and are benchmarked against systems without scheduling strategies under identical conditions.

1) Impact of Scheduling: To test the overall system performance of the scheduling and rateless coding, we randomly selected 20-time slices from the test set of the captured Wi-Fi data. Each time slice contains a total number of 24,000 data frames to be transmitted.

As shown in Fig. 10, it is found that, specifically, the BER decreases by approximately 29.7%; and transmission energy by approximately 6.8% on average. Throughput increases by approximately 2.5% on average. The utility factor increases by approximately 11.1% on average. The results indicate that using deep learning models for predictive scheduling significantly enhances the accuracy and efficiency of the system's transmission performance.

Idealistic scheduling conditions, serving as a benchmark for the system's optimal performance, result in an average decrease of 64.9% in BER and 12.5% in transmission energy, while throughput and utility increase by 6.1% and 21.6%, respectively, compared to no scheduling case. These results highlight the superiority of scheduling algorithms under optimal conditions.

Through comparative analysis, although predictive scheduling can not achieve the optimal results of idealistic scheduling, it still shows significant advantages over no scheduling conditions. Specifically, predictive scheduling exhibits noticeable decreases in key performance metrics such as BER, and transmission energy, while throughput and utility metrics also show significant improvements. This indicates that despite limitations in predictive accuracy, the overall performance of predictive scheduling outperforms the case without scheduling and approaches the best performance under idealistic scheduling conditions, validating the effectiveness and rationality of the predictive scheduling strategy. Although transmission time is slightly extended, it remains within an acceptable range, ensuring a balance between transmission efficiency and system reliability.

In summary, the experimental results demonstrate that the predictive scheduling strategy significantly improves system performance and efficiency compared to no scheduling. These findings validate the effectiveness of our proposed predictive scheduling strategy both in enhancing transmission accuracy and system throughput and assuring its rationality and potential in practical applications.

2) Comparative Analysis: To fully evaluate the performance of FlexScatter and demonstrate its advantages, we compare it with other state-of-the-art Wi-Fi backscatter systems. Table V presents the key features, including excitation signal type, scheduling strategies, energy efficiency and performance metrics.

Table V clearly indicates the advantages of FlexScatter compared to other existing Wi-Fi backscatter systems. Unlike traditional systems such as BackFi and Passive Wi-Fi, FlexScatter employs a predictive adaptive scheduling strategy that significantly improves energy efficiency and reduces BER by 30%. Moreover, it introduces an adaptive coding scheme to maintain reliability under dynamic Wi-Fi traffic conditions. These features allow FlexScatter to achieve a 7% increase in energy efficiency and an 11% improvement in utility, exhibiting the superiority over other state-of-the-art solutions.

3) Impact of Sites: After analyzing the Wi-Fi traffic data in three different scenarios: a shopping mall, a laboratory, and a residential apartment, it is found that the cumulative distribution function of the idle state of the excitation source fits the Pareto distribution, as shown in Fig. 3. Based on the collected Wi-Fi data, we estimate the Pareto distribution parameters α in these three scenarios, as shown in Table VI, where α represents the shape parameter of the Pareto distribution; the larger the α, the thinner the tail of the distribution, indicating a lower probability of large idle times.

To demonstrate the scheduling strategy's effectiveness, we generate packet intervals using the estimated Pareto distribution parameters with which we conducted simulations having 500 runs. Each simulation uses 5 milliseconds as a time slice, transmitting 100 frames per time slice.

As shown in Fig. 11, the scheduling strategy significantly improves performance metrics compared to the non-scheduling strategy in all three scenarios.

In the laboratory scenario, scheduling reduces the BER by 80%, from 0.1607 to 0.033, a fivefold improvement. Throughput increases by 7% (from 1.1869 to 1.2743), and utility improves by 22% (from 38.7053 to 47.1117).

In the residential scenario, scheduling reduces the average BER by 83%, from 0.0559 to 0.0092, a sixfold improvement. Throughput rises by 3% (from 1.2626 to 1.2981), and utility improves by 21% (from 59.7128 to 72.2397).

In the shopping mall scenario, scheduling reduces the average BER by 81%, from 0.1467 to 0.0278, a fivefold improvement. Throughput increases by 7% (from 1.1968 to 1.2774), and utility improves by 24% (from 36.4366 to 45.1348).

The differences in initial BER and the improvement levels of the scheduling strategy across different scenarios are closely

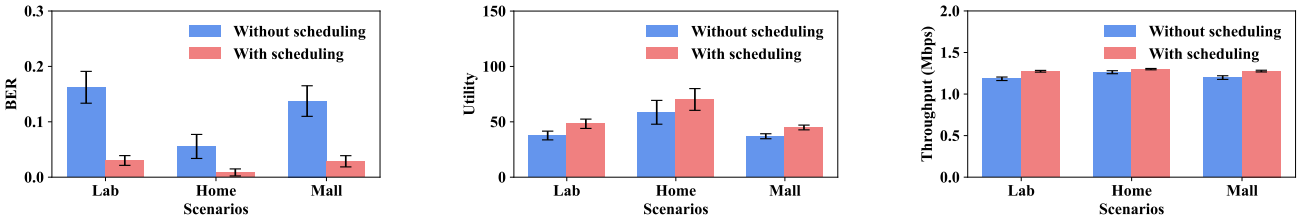

(a) BER (b) utility (c) throughput

Fig. 11. The performance with/without scheduling in three different scenarios using re-generated packets using Pareto distribution with the obtained parameters from the captured data.

TABLE V
COMPARISON OF WI-FI BACKSCATTER COMMUNICATION SYSTEMS

System	Excitation Signal	Scheduling Strategy	Energy Efficiency	Key Innovations	Performance Metrics	Complexity
FlexScatter	Unstable Wi-Fi signal	Predictive adaptive scheduling	Energy efficiency +7%	Predictive scheduling + adaptive coding for BER reduction	BER ↓ 30%, Utility ↑ 11%, Energy ↑ 7%	Low
BackFi	Wi-Fi signal	None	Low (backscatter dependent)	High-throughput backscatter using ambient Wi-Fi signals	1 Mbps (5m), 5 Mbps (1m)	Medium
Passive Wi-Fi	Ambient Wi-Fi signal	None (passive communication)	Ultra-high (microwatt level)	Ultra-low power 802.11b transmissions for IoT devices	14.5 μW @ 1 Mbps, 59.2 μW @ 11 Mbps, Range: 30-100 ft	Low
HitchHike	Wi-Fi signal	None (standard Wi-Fi support)	High (low-power backscatter)	Compatible backscatter modulation with standard Wi-Fi devices	Compatible with 802.11b Wi-Fi	Medium
GuardRider	Wi-Fi signal	Traffic-prediction-based	Moderate (depends on traffic)	Traffic prediction for optimized backscatter communication	Optimized for specific traffic models	High
RapidRider	Wi-Fi signal	OFDM symbol-level scheduling	High (efficient transmission)	Single-symbol backscatter + deinterleaving twins decoding	Max throughput: 235.3 kbps, 1.97x MOXcatter, 3.92x FreeRider	Medium
EEWScatter	Ambient Wi-Fi signal	None (system-wide energy design)	System power lowest	Low-power design + single-receiver decoding	System power: 1/3 of Passive WiFi, Tag power 1/1000 of radio	Medium

TABLE VI
PARETO DISTRIBUTION PARAMETERS FOR DIFFERENT SCENARIOS

Scenario	Channel	α
Laboratory	1	0.57
	6	0.54
	11	0.43
Shopping Mall	1	0.57
	6	0.54
	11	0.43
Residential Apartment	1	0.16
	6	0.09
	11	0.04

related to their environmental characteristics (see Table I). The shopping mall scenario, with its large area, high density of APs, and dynamic traffic patterns, experiences frequent collisions and interference, leading to the highest initial BER. In this complex environment, scheduling is essential for managing resource contention and significantly enhancing system performance.

In contrast, the laboratory scenario, characterized by moderate AP density, stable configurations and predictable traffic patterns, has a lower initial BER. The scheduling strategy optimizes traffic resource allocation and improves efficiency in this scenario.

The residential scenario, with minimal AP density and sparse traffic, has the lowest initial BER due to its low traffic demand. Even in this low-traffic environment, the scheduling strategy effectively enhances system reliability and reduces the waste of resources.

These findings demonstrate that the scheduling strategy is typically advantageous in high-traffic and dynamic environments, such as the shopping mall, while still delivering performance improvements in low-traffic settings, underscoring its adaptability and practicality across diverse scenarios.

V. DISCUSSIONS

Continuous and reliable Wi-Fi backscatter communication is critical for many practical applications. For instance, in health monitoring, real-time sensing of a patient's movement or breathing depends on uninterrupted signal transmission. Backscatter tags, which operate with minimal power consumption, must consistently transmit data to healthcare providers to ensure accurate and timely diagnosis. Any disruption in this communication can lead to incomplete data capture, delaying diagnosis or treatment and potentially compromising patient outcomes. Similarly, in logistics tracking, continuous backscatter communication ensures the precise monitoring of items in motion. Interruptions in communication can cause inventory discrepancies and shipment delays, particularly in dynamic environments like warehouses and distribution centers, where rapid and accurate updates are essential.

These examples underscore the importance of addressing the challenges associated with maintaining continuous Wi-Fi backscatter [28]. To tackle these issues, the proposed FlexScatter system introduces adaptive transmission scheduling and deep learning-based traffic prediction. These innovations allow the system to anticipate fluctuations in Wi-Fi traffic and dynamically adjust its transmission schedule, ensuring stable communication. By combining these predictive capabilities with energy-efficient operations, FlexScatter significantly enhances both the reliability and utility of backscatter systems in real-world applications.

The final model configuration for the traffic predictor demonstrates its suitability for resource-constrained IoT sce-

narios. With an input sequence length of 64, 8 features, 50 hidden units, and a step size of 5, the model achieves efficient performance with an inference complexity of approximately 1.7M FLOPs. This balance between computational efficiency and predictive accuracy ensures that the system meets the real-time traffic prediction requirement without overburdening the constrained hardware resources.

However, to minimize energy consumption, the current implementation of the traffic predictor processes data at the receiver, where predictions are computed and feedback is sent to the backscatter tag. This design reduces computational overhead on the low-power tag, enabling the system to operate within stringent energy limits. In future work, quantization methods will be explored to simplify the predictor, allowing for its potential deployment directly on the backscatter tag. This enhancement would enable real-time, on-tag adaptability to dynamic Wi-Fi conditions, improving the flexibility of our system and broadening its applicability to diverse IoT environments with limited resources.

VI. Conclusion

In this paper, we have proposed a novel deep learning-based traffic prediction and coding technique, FlexScatter, for Wi-Fi backscatter communications with uncontrolled traffic. The effectiveness and practicality of the coding and scheduling technique proposed in this paper have been verified through simulations with the aim of its application to the Wi-Fi backscatter communication systems. By leveraging deep learning-based traffic prediction, we have designed a scheduling algorithm which effectively identifies whether to transmit or to stay silent. Furthermore, we have proposed a rateless LDPC code to tackle the problem of dynamically varying channel conditions. It has been shown that the proposed system significantly enhances both reliability and efficiency. The improvements in terms of reliability and efficiency have been demonstrated not only in controlled laboratory environments but also in real-world application scenarios, to provide strong support for the deployment in diverse and complex settings.

References

[1] P. Zhang, C. Josephson, D. Bharadia, and S. Katti, "Freerider: Backscatter communication using commodity radios," in *Proceedings of the 13th International Conference on Emerging Networking EXperiments and Technologies*, ser. CoNEXT '17. New York, NY, USA: ACM, 2017, pp. 389–401. [Online]. Available: http://doi.acm.org/10.1145/3143361.3143374

[2] M. Y. Onay and B. Dulek, "Performance analysis of TV, FM and WiFi signals in backscatter communication networks," in *2019 27th Signal Processing and Communications Applications Conference (SIU)*. IEEE, 2019, pp. 1–4.

[3] V. Liu, A. Parks, V. Talla, S. Gollakota, D. Wetherall, and J. R. Smith, "Ambient backscatter: Wireless communication out of thin air," in *Proceedings of the ACM SIGCOMM 2013 Conference on SIGCOMM*, ser. SIGCOMM '13. New York, NY, USA: ACM, 2013, pp. 39–50. [Online]. Available: http://doi.acm.org/10.1145/2486001.2486015

[4] J. Rosenthal and M. S. Reynolds, "A 158 pj/bit 1.0 mbps bluetooth low energy (BLE) compatible backscatter communication system for wireless sensing," in *2019 IEEE Topical Conference on Wireless Sensors and Sensor Networks (WiSNet)*. IEEE, 2019, pp. 1–3.

[5] J. Huang, G. Xing, G. Zhou, and R. Zhou, "Beyond co-existence: Exploiting WiFi white space for zigbee performance assurance," in *The 18th IEEE International Conference on Network Protocols*. IEEE, 2010, pp. 305–314.

[6] V. Talla, M. Hessar, B. Kellogg, A. Najafi, J. R. Smith, and S. Gollakota, "LoRa backscatter: Enabling the vision of ubiquitous connectivity," *Proc. ACM Interact. Mob. Wearable Ubiquitous Technol.*, vol. 1, no. 3, pp. 105:1–105:24, Sep. 2017. [Online]. Available: http://doi.acm.org/10.1145/3130970

[7] Y. Peng, L. Shangguan, Y. Hu, Y. Qian, X. Lin, X. Chen, D. Fang, and K. Jamieson, "PLoRa: A passive long-range data network from ambient loRa transmissions," in *Proc. of ACM SIGCOMM*. New York, NY, USA: ACM, 2018, pp. 147–160.

[8] A. Wang, V. Iyer, V. Talla, J. R. Smith, and S. Gollakota, "FM backscatter: Enabling connected cities and smart fabrics," in *Proc. of USENIX NSDI*. Boston, MA: USENIX Association, 2017, pp. 243–258.

[9] D. Bharadia, K. R. Joshi, M. Kotaru, and S. Katti, "BackFi: High throughput WiFi backscatter," in *Proceedings of the 2015 ACM Conference on Special Interest Group on Data Communication*, ser. SIGCOMM '15. New York, NY, USA: ACM, 2015, pp. 283–296. [Online]. Available: http://doi.acm.org/10.1145/2785956.2787490

[10] B. Kellogg, A. Parks, S. Gollakota, J. R. Smith, and D. Wetherall, "Wi-Fi backscatter: Internet connectivity for RF-powered devices," in *Proceedings of the 2014 ACM Conference on SIGCOMM*, ser. SIGCOMM '14. New York, NY, USA: ACM, 2014, pp. 607–618. [Online]. Available: http://doi.acm.org/10.1145/2619239.2626319

[11] B. Kellogg, V. Talla, J. R. Smith, and S. Gollakot, "PASSIVE WI-FI: Bringing low power to Wi-Fi transmissions," in *Proc. of USENIX NSDI*. USENIX Association, March 2016, pp. 151–164.

[12] P. Zhang, D. Bharadia, K. Joshi, and S. Katti, "HitchHike: Practical backscatter using commodity WiFi," in *Proceedings of the 14th ACM Conference on Embedded Network Sensor Systems CD-ROM*, ser. SenSys '16. New York, NY, USA: ACM, 2016, pp. 259–271. [Online]. Available: http://doi.acm.org/10.1145/2994551.2994565

[13] T. Kim and W. Lee, "Exploiting residual channel for implicit wi-Fi backscatter networks," in *IEEE INFOCOM 2018 - IEEE Conference on Computer Communications*, April 2018, pp. 1–9.

[14] C. Yang, J. Gummeson, and A. Sample, "Riding the airways: Ultra-wideband ambient backscatter via commercial broadcast systems," in *IEEE INFOCOM 2017 - IEEE Conference on Computer Communications*, May 2017, pp. 1–9.

[15] J. Zhao, W. Gong, and J. Liu, "X-Tandem: Towards multi-hop backscatter communication with commodity WiFi," in *Proceedings of the 24th Annual International Conference on Mobile Computing and Networking*, ser. MobiCom '18. New York, NY, USA: ACM, 2018, pp. 497–511. [Online]. Available: http://doi.acm.org/10.1145/3241539.3241553

[16] Z. Huang, Y. Ding, D. O. Wu, S. Wang, and W. Gong, "Bitalign: Bit alignment for bluetooth backscatter communication," *IEEE Transactions on Mobile Computing*, 2024.

[17] R. B. Nti, D. K. P. Asiedu, and J.-H. Yun, "Nonsequential link adaptation using repetition codes for Wi-Fi backscatter communication," *IEEE Transactions on Vehicular Technology*, 2024.

[18] X. He, W. Jiang, M. Cheng, X. Zhou, P. Yang, and B. Kurkoski, "Guardrider: Reliable WiFi backscatter using reed-Solomon codes with QoS guarantee," in *2020 IEEE/ACM 28th IWQoS*, 2020, pp. 1–10.

[19] Z. Yang, X. He, G. Lin, W. Jiang, Y. Zhu, J. Sun, Y. Xu, and P. Yang, "Nuwa: off-state tolerant backscattering system with uncontrolled excitation traffics," *Journal of Cloud Computing*, vol. 12, no. 1, Nov. 2023. [Online]. Available: http://dx.doi.org/10.1186/s13677-023-00508-5

[20] G. Yang, Q. Zhang, and Y.-C. Liang, "Cooperative ambient backscatter communications for green internet-of-things," *IEEE Internet of Things Journal*, vol. 6, no. 2, pp. 2612–2625, 2019.

[21] Q. Wang, S. Chen, J. Zhao, and G. Wei, "Rapidrider: Efficient wifi backscatter with uncontrolled ambient signals," in *Proc. of IEEE INFOCOM*. Virtual Conference: IEEE, 2021, pp. 1–10.

[22] R. Li, Z. Zhao, J. Zheng, C. Mei, Y. Cai, and H. Zhang, "The learning and prediction of application-level traffic data in cellular networks," *IEEE Transactions on Wireless Communications*, vol. 16, no. 6, pp. 3899–3912, 2017.

[23] F. Xu, Y. Lin, J. Huang, D. Wu, H. Shi, J. Song, and Y. Li, "Big data driven mobile traffic understanding and forecasting: A time series approach," *IEEE transactions on services computing*, vol. 9, no. 5, pp. 796–805, 2016.

[24] N. Wang, B. Li, M. Yang, Z. Yan, and D. Wang, "Traffic arrival prediction for wifi network: A machine learning approach," in *International Conference on Internet of Things as a Service*. Springer, 2019, pp. 480–488.

[25] H. D. Trinh, L. Giupponi, and P. Dini, "Mobile traffic prediction from raw data using lstm networks," in *2018 IEEE 29th annual international symposium on personal, indoor and mobile radio communications (PIMRC)*. IEEE, 2018, pp. 1827–1832.

[26] N. Ramakrishnan and T. Soni, "Network traffic prediction using recurrent neural networks," in *2018 17th IEEE International Conference on Machine Learning and Applications (ICMLA)*. IEEE, 2018, pp. 187–193.

[27] S. Rostami, H. D. Trinh, S. Lagen, M. Costa, M. Valkama, and P. Dini, "Proactive wake-up scheduler based on recurrent neural networks," in *ICC 2020-2020 IEEE International Conference on Communications (ICC)*. IEEE, 2020, pp. 1–6.

[28] V. Talla, J. Smith, and S. Gollakota, "Advances and open problems in backscatter networking," *GetMobile: Mobile Comp. and Comm.*, vol. 24, no. 4, p. 32–38, Mar. 2021. [Online]. Available: https://doi.org/10.1145/3457356.3457367